JOURNAL OF SYNCHROTRON RADIATION

ISSN 1600-5775

Spherical micro-hole grid for high-resolution retarding field analyzer

Takayuki Muro,[a]* Tomohiro Matsushita,[b] Kazumi Sawamura[c] and Jun Mizuno[d]

[a]Japan Synchrotron Radiation Research Institute (JASRI), 1-1-1 Kouto, Sayo, Hyogo 679-5198, Japan, [b]Graduate School of Science and Technology, Nara Institute of Science and Technology, 8916-5 Takayama, Ikoma, Nara 630-0192, Japan, [c]IMUZAK Inc., 2-2-1 Matsuei, Yamagata-shi, Yamagata 990-2473, Japan, and [d]Research Organization for Nano and Life Innovation, Waseda University, 513 Wasedatsurumaki, Shinjuku, Tokyo 162-0041, Japan.
*Correspondence e-mail: muro@spring8.or.jp

Received 1 June 2021
Accepted 29 July 2021

Edited by I. Lindau, SLAC/Stanford University, USA

Keywords: retarding field analyzers; spherical grids; micro cylindrical holes; photoelectron holography.

A wide-acceptance-angle spherical grid composed of numerous micro cylindrical holes was developed to be used for the retarding grid of a display-type retarding field analyzer (RFA) and to enhance the energy resolution ($E/\Delta E$). Each cylindrical hole with a diameter of 50 µm and a depth of 80 µm is directed to the spherical center. The inner radius of the spherical grid is 40 mm. The holed area corresponds to an acceptance angle of ±52°. The $E/\Delta E$ of an RFA equipped with the developed holed grid was estimated to be 2000 from a measured Au 4*f* photoemission spectrum. A clear photoelectron hologram was observed in the Mo 4*p* core-level region of MoS_2, indicating that the RFA with the holed grid is effective for photoelectron holography.

1. Introduction

Retarding field analyzers (RFAs) composed of spherical grids can be used as two-dimensional angle-resolved photoelectron energy analyzers (Kanayama *et al.*, 1989). However, the typical resolving power ($E/\Delta E$) of a traditional three-grid RFA is ∼100 (Taylor, 1969) and too low for photoelectron diffraction or photoelectron holography (Matsushita *et al.*, 2010). We previously reported on a grid arrangement enhancing the $E/\Delta E$ (Muro *et al.*, 2017). In the improved arrangement, the distance between the first and second grids is much longer than that between the second and third grids, as shown in Fig. 1(*a*), whereas the distances are the same in most of the cases of conventional RFAs. An RFA developed at BL25SU (Senba *et al.*, 2016) of SPring-8 employing the improved arrangement showed an $E/\Delta E$ of 1100 (Muro *et al.*, 2017). The radii of the first, second and third grids were 12, 40 and 42 mm, respectively. A woven tungsten mesh with a mesh number of 250 was used for the second grid, *i.e.* the retarding grid. The photoelectron acceptance angle was ±49°, which was limited by the diameter of the detector shown in Fig. 1(*a*). Our simulation also predicted that the $E/\Delta E$ can further be enhanced when the mesh retarding grid is replaced by a partial spherical shell like a dome with radially directed cylindrical holes, as schematically shown in Fig. 1(*b*). Hereafter, we call such a grid a holed grid. We tentatively fabricated a holed grid with a small holed area corresponding to an acceptance angle of ±7°. The diameter of a cylinder was 60 µm and the depth, *i.e.* the thickness of the spherical shell, was 100 µm. The distance between the center positions of two neighboring holes, *i.e.* the pitch of the holes, was ∼100 µm. The inner radius of the spherical shell was 40 mm, which was the same as the mesh retarding grid. The RFA equipped with the holed grid

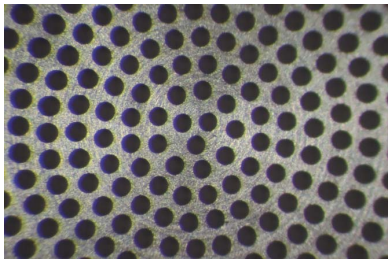

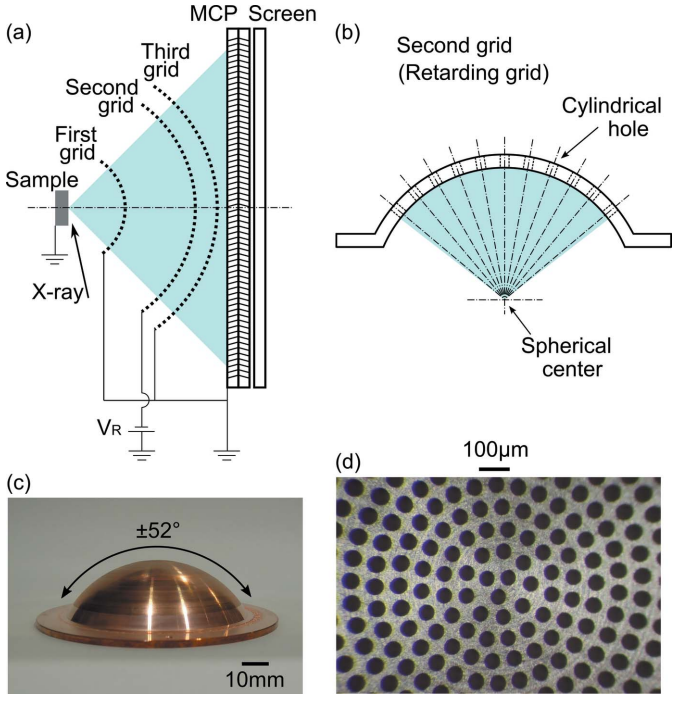

Figure 1
(*a*) A schematic of the display-type three-grid RFA employing the improved grid arrangement. (*b*) A schematic of the partial spherical shell with radially directed cylindrical holes used for the second grid, *i.e.* the retarding grid. (*c*) A photograph of the fabricated partial spherical shell with a holed area corresponding to an acceptance angle of ±52°. (*d*) A zoomed-in photograph of the holed area on the inner side of the spherical shell.

showed a high $E/\Delta E$ of 1800 (Muro *et al.*, 2017). Our remaining challenge was to expand the holed area to be larger than the acceptance angle of ±49° determined by the detector. In this article, we report on a holed grid with a wide holed area corresponding to an angle of ±52° and the results of some evaluation measurements using synchrotron radiation.

2. Spherical grid composed of micro cylindrical holes

Figs. 1(*c*) and 1(*d*) are photographs of the fabricated holed grid. The material is copper. The thickness of the spherical shell is 80 μm. The inner radius of the spherical shell is 40 mm, which is the same as the retarding grid of the previously developed RFA (Muro *et al.*, 2017). The cylindrical holes were manufactured by drilling. The diameter of a cylinder is 50 μm. As shown in Fig. 1(*b*), the center axis of each cylinder is directed to the spherical center. The pitch of the holes is ∼70 μm. As indicated in Fig. 1(*c*), the holed area corresponds to an acceptance angle of ±52°, resulting in the total hole number of ∼800 000. Assuming a triangle lattice arrangement of the holes, the transmittance is expected to be ∼45%. However, from Fig. 1(*d*), the transmittance of the fabricated holed grid is estimated to be ∼35% due to the deviation from the triangle lattice. The transmittance of the 250 mesh previously used was 65% (Muro *et al.*, 2017).

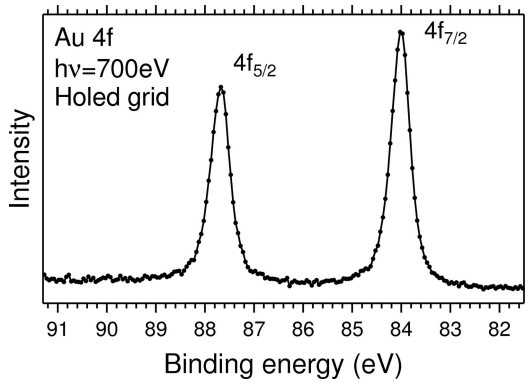

Figure 2
An Au 4*f* photoemission spectrum of evaporated gold measured by the RFA with the holed retarding grid shown in Fig. 1(*c*). The excitation photon energy was 700 eV. The sample was at room temperature.

3. Results of evaluation measurements

For evaluation measurements, we replaced the retarding grid of the previously developed RFA (Muro *et al.*, 2017) with the newly fabricated holed grid. The measurements were performed at the soft X-ray beamline BL25SU (Senba *et al.*, 2016) of SPring-8. Fig. 2 shows an Au 4*f* photoemission spectrum of evaporated gold measured by the RFA equipped with the holed grid. The photon energy of the excitation beam was 700 eV. The ΔE of the beamline monochromator was set to 82 meV. The beam spot size on the sample surface was ∼5 μm × 70 μm. The sample was at room temperature. By comparing the spectrum in Fig. 2 with that measured by a concentric hemispherical analyzer with a known ΔE (Muro *et al.*, 2017), we estimated the $E/\Delta E$ of the RFA with the holed grid to be 2000, which is even higher than the previous value of 1800 obtained by the narrow-acceptance holed grid (Muro *et al.*, 2017). As already mentioned, the transmittance of the present holed grid is ∼35%, whereas that of the 250 mesh is 65%. We previously confirmed that clear photoelectron holograms can be observed using the RFA with the 250-mesh retarding grid (Muro *et al.*, 2017). However, the acceptance angle of the previous holed grid was too narrow for observing photoelectron holograms. Fig. 3(*b*) shows the result of a photoelectron-hologram measurement in the Mo 4*p* core-level region of MoS_2 by the RFA with the present holed grid. The excitation photon energy was 700 eV. The MoS_2 sample was cleaved in air before the measurement. The sample was at room temperature during the measurement. As shown in Fig. 3(*b*), a clear hologram pattern was observed. For comparison, Fig. 3(*a*) shows the result obtained by the RFA with the 250-mesh retarding grid. The measurement conditions including the beamline setting and the measurement time were the same between Figs. 3(*a*) and 3(*b*). Despite the lower transmittance of the holed grid, the clearness of the hologram pattern in Fig. 3(*b*) is comparable with that in Fig. 3(*a*). This indicates that the holes are sufficiently small and dense so as not to affect the angular resolution of the RFA. It should be mentioned that the beam spot size also affects the angular as well as energy resolutions of an RFA.

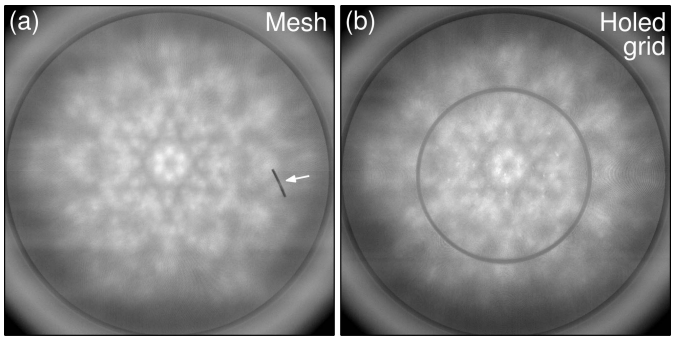

Figure 3
Mo 4*p* photoelectron holograms of MoS_2 measured by (*a*) the RFA with the 250-mesh retarding grid and (*b*) the RFA with the holed retarding grid shown in Fig. 1(*c*). The energy window was ±5 eV including the Mo 4*p* photoemission peak. The excitation photon energy was 700 eV. The sample was at room temperature. The acceptance angle was ±49°. The acceptance angle was limited by the diameter of the detector in spite of the larger acceptance of ±52° of the holed grid. The line-shaped defect indicated by an arrow in (*a*) was caused by dust on the detector. This dust was removed before the measurement of (*b*). For the reason for the ring-shaped defect seen in (*b*), see the main text.

Roughly speaking, spot sizes ≤100 µm are favorable for the RFA presented here. The beam spot size on the sample for the measurements of Fig. 3 was ∼55 µm × 70 µm, which is larger than the size for Fig. 2 because of the grazing incidence to the sample. In Fig. 3(*b*), the moiré pattern caused by the combination of the three grids seems to be relatively prominent compared with that in Fig. 2(*a*). The moiré pattern could be suppressed by changing the relative rotation angles between the three grids (Matsushita *et al.*, 2020). One may notice that there are small bright spots in the central region in Fig. 3(*b*). On the outer side surface of the holed grid, there are unwanted small dents, which were formed in the manufacturing process. We suppose that these dents locally distorted the electric fields and worked as lenses for electrons forming the bright spots. The dents can be eliminated in the next fabrication by improving the manufacturing process. Unfortunately, a ring-shaped shaded area was observed in Fig. 3(*b*), where drilling was not completed and the hole openings are almost closed at the ends of the cylinders. Because the wear of a drill is inevitable, the drill has to be replaced at regular time intervals. The ring-shaped defect area was due to a setting error of a drill, which can also be eliminated in the next fabrication.

4. Outlook

In this work, we confirmed that an RFA equipped with a retarding grid composed of micro cylindrical holes is effective for photoelectron holography. Unfortunately, the holed grid reported in this article had a ring-shaped defect area. Based on this result, we improved the manufacturing process and are planning to fabricate a new holed grid with an even higher transmittance. In the near future, we will report on photoelectron holograms measured by using the new holed grid without any defect areas.

Acknowledgements

The authors are grateful to Takumi Kamibayashi for his support on the development of the spherical grid. The synchrotron radiation experiments were performed with the approval of JASRI (Proposal Nos. 2019A1323, 2019A2067, 2019B2028 and 2020A2048).

Funding information

This work was supported by the Japan Society for the Promotion of Science KAKENHI Grant Nos. JP16K13733 and JP17H06201.

References

Kanayama, S., Owari, M., Nakamura, E. & Nihei, Y. (1989). *Rev. Sci. Instrum.* **60**, 2231–2234.
Matsushita, T., Matsui, F., Daimon, H. & Hayashi, K. (2010). *J. Electron Spectrosc. Relat. Phenom.* **178–179**, 195–220.
Matsushita, T., Muro, T., Matsui, F., Happo, N. & Hayashi, K. (2020). *Jpn. J. Appl. Phys.* **59**, 020502.
Muro, T., Ohkochi, T., Kato, Y., Izumi, Y., Fukami, S., Fujiwara, H. & Matsushita, T. (2017). *Rev. Sci. Instrum.* **88**, 123106.
Senba, Y., Ohashi, H., Kotani, Y., Nakamura, T., Muro, T., Ohkochi, T., Tsuji, N., Kishimoto, H., Miura, T., Tanaka, M., Higashiyama, M., Takahashi, S., Ishizawa, Y., Matsushita, T., Furukawa, Y., Ohata, T., Nariyama, N., Takeshita, K., Kinoshita, T., Fujiwara, A., Takata, M. & Goto, S. (2016). *AIP Conf. Proc.* **1741**, 030044.
Taylor, N. J. (1969). *Rev. Sci. Instrum.* **40**, 792–804.